Flame Retarded Epoxy Resins by Adding Layered Silicate in Combination with the Conventional Protection-Layer-Building Flame Retardants Melamine Borate and Ammonium Polyphosphate

B. Schartel,[1] A. Weiß,[1] F. Mohr,[2] M. Kleemeier,[2] A. Hartwig,[2] U. Braun[1]

[1]*BAM Federal Institute for Materials Research and Testing, Unter den Eichen 87, Berlin 12205, Germany*
[2]*Fraunhofer Institute for Manufacturing Technology and Applied Materials Research, Wiener Str. 12, Bremen 28359, Germany*

Received 8 June 2009; accepted 25 March 2010
DOI 10.1002/app.32512
Published online 28 May 2010 in Wiley InterScience (www.interscience.wiley.com).

ABSTRACT: The pyrolysis and flammability of phosphonium-modified layered silicate epoxy resin nanocomposites (EP/LS) were evaluated when LS was combined with two flame retardants, melamine borate (MB) and ammonium polyphosphate (APP), that also act via a surface protection layer. Thermogravimetry (TG), TG coupled with Fourier Transform Spectroscopy (TG-FTIR), oxygen index (LOI), UL 94 burning chamber (UL 94) and cone calorimeter were used. The glassy coating because of 10 wt % MB during combustion showed effects in the cone calorimeter test similar to nanodispersed LS, and somewhat better flame retardancy in flammability tests, such as LOI and UL 94. Adding APP to EP resulted in intumescent systems. The fire retardancy was particularly convincing when 15 wt % APP was used, especially for low external heat flux, and thus, also in flammability tests like LOI and UL 94. V0 classification is achieved when 15 wt % APP is used in EP. The flame retardancy efficiency of the protection layers formed does not increase linearly with the MB and APP concentrations used. The combination of LS with MB or APP shows antagonism; thus the performance of the combination of LS with MB or APP, respectively, was disappointing. No optimization of the carbonaceous-inorganic surface layer occurred for LS-MB. Combining LS with APP inhibited the intumescence, most probably through an increase in viscosity clearly above the value needed for intumescent behavior.
 J Appl Polym Sci 118: 1134–1143, 2010

Key words: nanocomposites; fire retardance; thermosets; organoclay; ammonium polyphosphate; melamine borate

INTRODUCTION

Polymer nanocomposites have been proposed as an up-and-coming approach to flame retardant polymeric materials.[1] They are made available with established and thus economical preparation tools, such as extrusion and injection molding for thermoplastics, but also through *in situ* polymerization for thermosets. Indeed, their commercial use in mass products has become an accepted method to improve mechanical properties[2,3] as a kind of cheap molecular reinforcement[4] but also to reduce fire hazards.[5] Because of their positive impact on mechanical properties and their ecofriendly characteristics they are discussed as a halogen-free alternative to established flame retardants. Comparing nanocomposites with microcomposites makes clear that this technology aims beyond "simple" further miniaturization. It is based on the exploitation of new effects that arise from nanostructured materials, surface-controlled mechanisms, and the use of single homogeneous particles without defects.

Several effects are underlined to characterize the flame retardancy mechanisms of nanocomposites[6–14]: formation of a homogeneous silicate-carbonaceous char residue layer that works as heat shield during burning, increasing the viscosity of the melt to reduce dripping, melt flow and bubbling, catalytic impacts increasing the char yield and changing the products, and reducing the permeation to lower mass and oxygen transport. The characteristics of the two main general flame retardancy mechanisms in nanocomposites—formation of a silicate-carbonaceous char residue layer and increasing the viscosity—explain why the use of nanoparticles alone generally is not sufficient to flame retard polymeric materials.[10,15] Nanocomposites show deficits in fire load reduction (total heat evolved, THE) and in fire scenarios with a lower external impact, such as flammability tests based on the reaction to a small flame (for instance UL 94). Thus, the combination of the nanocomposite approach with established flame

Correspondence to: B. Schartel (bernhard.schartel@bam.de).

Contract grant sponsor: German Research Foundation (DFG); contract grant number: Scha 730/8-1, Scha 730/8-2, Ha 2420/6-1, Ha 2420/6-2.

retardants is proposed and reviewed.[16–19] Such systems are not only promising with respect to increasing flame retardancy efficiency, to avoid the concomitant deteriorating impact on other properties like mechanical properties or to enable the reduction of additive content, some of them also have been commercialized successfully because of such key benefits.[20,21] Contrary to nanocomposites, such combinations of nanocomposites with established flame retardants have been reported to show promise with respect to industrial exploration. Thus, it is not astonishing that, from the very beginning, patents proposed combinations with flame retardants like phosphates and red phosphorus.[20–25] Analogous ideas have been addressed since then by various groups.[26–29] The combination with intumescent formulations, and in particular with ammonium polyphosphate (APP), has been studied and is reported to show synergistic effects.[30–32] The combinations with metal hydroxides are very successful.[21,33–35] Also, combinations with melamine-based and halogen-containing flame retardants have been reported.[36,37] By now a great number of different combinations have been addressed at least to some extent. Nevertheless, an infinite number of possibilities and potential approaches result from screening or optimization of the kinds and amounts of polymer, nanoparticles, modifiers/compatibilizers, flame retardant, and additional components. It is high time to evaluate the characteristic phenomena of specific approaches and assess the corresponding concepts rather than merely investigating one specific nanocomposite conventional flame retardant combination after the other.

This work focuses on combining nanodispersed layered silicate with flame retardants that also act via a surface protection layer. In particular the question is addressed as to whether the surface effects enhance or compete with each other. Phosphonium-modified layered silicate (LS) epoxy resin (EP) nanocomposites[19,38,39] in combination with melamine borate (MB) and APP were evaluated. Both MB and APP are additives, which are used to flame retard polymeric materials and are believed to act by building up a protective surface layer. Borates tend to form glassy coatings. APP is used as a key agent for many intumescent systems. The formation of a carbon-silicate layer is the main flame retardancy impact of layered silicate nanocomposite. The combination of the additives is interesting, particularly since the flame retardancy efficiency of the protection layers formed does not increase linearly with the concentration of the additives used.[10,40] Thus, the combination may be a way to achieve a level of protection that is not possible by increasing the amount of additives. Further, it is the aim of this work to address the interdependence between the different mechanisms. As the condensed-phase mechanisms at the top of the burning material play the important role for all three additives, interactions resulting in synergism or antagonism are expected.

EXPERIMENTAL PART

Materials

Tetraphenyl phosphonium-modified layered silicate (LS) epoxy resin (EP) nanocomposites (EP/LS, always 5 wt % LS was used), and these nanocomposites in combination with 5 wt % MB (EP/LS/5MB) and 10 wt % APP (EP/LS/10APP) were evaluated and compared to EP, as well as to EP/5MB, EP/10MB (EP/10 wt % MB), EP/10APP and EP/15APP (EP/15 wt % APP). The compositions and abbreviations used for the different samples containing the various fillers are summarized in Table I. The EP consisted of a bisphenol A diglycidylether-based epoxy resin (Araldit GY 250, Huntsman) cured with an equimolar amount of 4-methyl hexahydrophthalic anhydride (MHHPA, Acros Organics). The curing reaction was accelerated by 1 wt % 1-methylimidazole (1-MI, Aldrich). The LS was produced by exchanging the sodium ions of the bentonite Nanofill 757 (Südchemie, cation exchange capacity of 0.8 mmol g^{-1}) with equimolar amounts of tetraphenyl phosphonium bromide (Evonik-Degussa). By using the equimolar amount no excess surfactant was obtained. Ammonium-based bromide and using significant excess surfactant are common in commercial systems. Tetraphenyl phosphonium and such low amount of surfactant was used to rule out a worsening of thermal stability and time to ignition.[19,38,41,42] After washing out the NaBr the dispersion was spray-dried with a Büchi Mini Spray Dryer B-290. The LS obtained by this procedure had a specific surface area of 93 m^2 g^{-1}, as determined by the nitrogen absorption method (BET surface area). A more detailed description of the preparation of LS and its incorporation in the epoxy resin has been published elsewhere.[19] The melamine borate (MB) used for this work had a mean particle diameter D_{50} of 15 μm (Budit 313, Budenheim). APP was obtained from Clariant (Exolit AP 423, D_{50} = 8 μm). Both flame retardants were dispersed in the composite of LS and epoxy resin using a dissolver (CA 40, VMA Getzmann). The mixtures were stirred with a dissolver blade (60 mm diameter) for 1 h at 1500 rpm and 50°C. After addition of hardener (MHHPA) and accelerator (1-MI), the reactive mixture was homogenized and cast into a preheated aluminummold (250× 200 × 5 mm) coated with Acmosan 82–7203 (Acmos Chemie) as a mold-release agent. Samples were cured for 1 h at 120°C and cut into the testing specimen afterward. The chosen curing time and

TABLE I
Composition (in wt %) and Assignment of the Investigated Samples

In wt %	EP	LS	APP	MB
EP	100			
EP/LS	95	5		
EP/10APP	90		10	
EP/LS/10APP	85	5	10	
EP/15APP	85		15	
EP/5MB	95			5
EP/LS/5MB	90	5		5
EP/10MB	90			10

temperature result in a rather complete curing reducing any differences between the different systems. Differential scanning calorimeter (DSC) investigations on the cured samples showed curing peaks of 19.6 J g^{-1} for EP and 14.4 J g^{-1} for EP/LS, which corresponds to 5.4 and 4.0%, respectively, of the curing enthalpy of the complete curing (360 J g^{-1}). Thus the curing was nearly completed (around 95%) with a difference smaller than 1.5% between EP and EP/LS due to incorporation of LS. The glass transition temperature of EP was 167°C the one of EP/LS 156°C. Whereas, the DSC results indicated somewhat surprisingly an even slightly higher crosslinking, the small reduction in glass transition temperature is commonly interpreted as indicator for a reduced crosslinking. However, strictly speaking the glass transition temperature is not a biunique indicator. The reduction can also be due to a change in free volume or molecular interactions by the incorporated filler. The morphology of the composites was determined using X-ray, scanning electron microscopy (SEM), and transmission electron microscopy (TEM) investigations.

Electron microscopy

The samples for the TEM investigations were prepared in epoxy resin and cut into ca. 100-nm thick slices with a Leica Ultracut UCT equipped with a diamond knife. The samples were examined with the TEM TECNAI G2 from FEI.

Thermal analysis

The thermal and thermo-oxidative decomposition and the evolved gas during pyrolysis were studied by means of TG–FTIR (Thermobalance TGA/STDA 851 by Mettler-Toledo, Gießen, Germany coupled with the FTIR-Spectrometer Nexus 470 by Nicolet Instruments, Offenbach, Germany).[43] A heating rate of 10°C min^{-1} and a nitrogen or air flow of 30 cm^3 min^{-1} were used. The sample mass was about 10–12 mg. The transfer line between the thermobalance and the FTIR spectrometer had an inner diameter of 1 mm. The transfer line and the FTIR cell were heated to 250°C. The optical path length of the FTIR cell was 20 cm. A resolution of 4 cm^{-1} was used based on a scan rate of 16 and recording frequency of spectra every 8 s.

Fire testing

The response to a small flame (flammability) was investigated by means of both the limiting oxygen index (LOI) following ISO 4589 and the UL 94 test in the vertical and horizontal configuration according to IEC 60,695-11-10. The fire behavior under forced flaming conditions was investigated with a cone calorimeter[44] according to ISO 5660 in the horizontal sample position using the retainer frame. External heat fluxes (irradiation) of 35, 50 and 70 kW m^{-2} were applied. All cone calorimeter tests were performed in duplicate or triplicate.

RESULTS AND DISCUSSION

The composites' morphology

The strong impact of the nanocomposite morphology on the fire behavior of the investigated EP/LS system was reported before.[19,45] Thus, the morphology of the composites was determined using three different methods: X-ray, SEM, and TEM. The results constituted a consistent picture of the materials morphology that is best illustrated by the TEM results for different magnifications (Fig. 1). Actually, only the TEM results illustrate the different features necessary to describe the morphology satisfactory, whereas the SEM and X-ray results did support this picture mainly by putting forward no objection. The morphology of EP/LS clearly differed from a microcomposite. Nevertheless, the silicate layers in the composites showed neither simple dispersion nor simple exfoliation or one of these phenomena in a perfect manner. What is more, the morphology is characterized satisfactorily only by discussing it on different length scales. On the large scale, LS-rich phases, EP/LS agglomerates with sizes in the micron range, are formed within EP. This characteristic is shown in Figure 1(a) for the example of the EP/LS composite. At higher magnification it becomes obvious that the agglomerates are not compact as expected for microcomposites, but consist of a loose network of silicate layers, which is infiltrated by the epoxy resin [Fig. 1(b, c)]. Therefore, the morphology of the sample can best be described as blend of nanostructured microparticles embedded in the polymer matrix. At higher magnifications it becomes clear that the nanostructured microparticles are characterized by typical nanocomposite morphology. Nanoparticles consisting of stacks of only 2–20

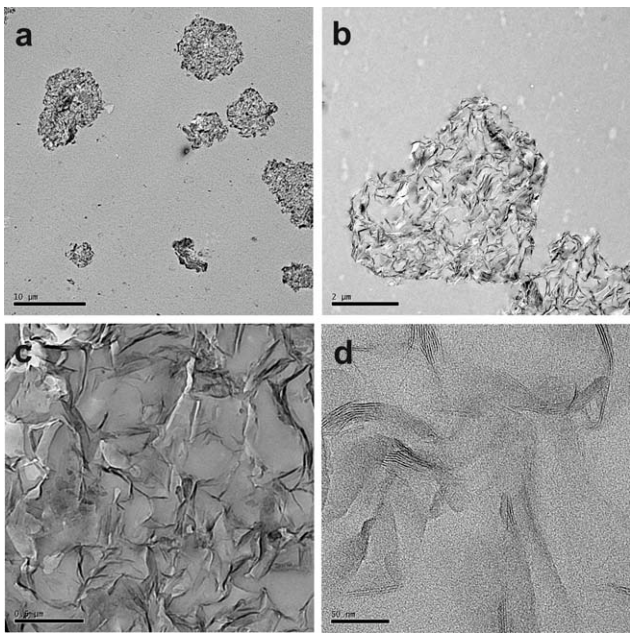

Figure 1 EP/LS morphology illustrated by TEM at different magnifications (the bar in $a = 10$ μm; in $b = 2$ μm; in $c = 0.5$ μm; in $d = 50$ nm). (a) and (b) show the nanostructured microparticles embedded in EP; (c) and (d) the nanocomposite morphology of the microparticles.

silicate layers embedded by EP are observed [Fig. 1(d)]. X-ray results showed a broadened and reduced peak, and thus, confirm the reduction of the layered silicate stacks. It should be noted that this special kind of nanocomposite morphology shows an extremely large interphase between layered silicate sheets and EP, very similar to better-dispersed nanocomposite morphology.

Thermal decomposition

Under inert atmosphere EP decomposes in one major decomposition step, with a mass loss (ML) of around 90 wt % and $T_{max} = 410$°C (T_{max} = temperature for the maximum in ML rate) (Fig. 2 and Table II). During the major decomposition step, volatiles in FTIR were identified by characteristic signals of dicarbonic acids, such as butandioic acid (3577, 1872, 1810, 1121, and 1051 cm^{-1}), carbonyl or ketone species (1730 cm^{-1}), phenolic derivatives (3650, 1608, 1512, 1257, 1174 cm^{-1}), CH_4 (sharp peak at 3015 cm^{-1}), CO_2 (2357 and 2309 cm^{-1}), and CO (2175 and 2126 cm^{-1}). No chronology in the release of the different products was unambiguously monitored. The sharp decomposition step resulted in an almost simultaneously release of the different volatiles. The peaks of product release rate versus time or temperature, respectively, overlapped strongly. The differences between the times to maximum release rate were less than 1.5 min or 10 K, respectively, comparing the different products. Small products, such as CO, seemed to be released early. However, this may also be due to smaller volatile specific transfer times into the FTIR gas cell. The residues at 500°C and 850°C were between 5.4 and 3.9 wt %. Adding LS to EP has a minor influence on the thermal decomposition of the EP (Fig. 2). Only the beginning of decomposition is enhanced, shown by the reduction of 22°C in $T_{5\%}$ ($T_{5\%}$ = temperature for 5 wt % ML). Volatiles and T_{max} were not changed at all. The inorganic part of LS resulted in an increase in residue of around 4.4–3.8 wt %. Apart from the impact on the beginning of decomposition, LS behaves like an inert filler in EP. Also, adding MB mainly influences the beginning of the decomposition. $T_{5\%}$ was decreased by 70°C for EP/5MB and 90°C for EP/10MB, respectively, whereas T_{max} was still observed very close to the EP decomposition (difference < 8°C). The volatiles equalled the results for EP, apart from some minor additional signals at 3450 cm^{-1}, 1758 cm^{-1}, and 1326 cm^{-1}, which were caused by additional amide species. These species indicated some aminolysis reaction of melamine with dicarbonic acid such as with butandioic acid to butanamide. The resulting formation of cyanuric acid was observed through signals of isocyanic acid at 2250 cm^{-1}. The residue at 500°C was increased by 8.1 wt % when 5 wt % MB was added, and 12 wt % when 10 wt % MB was added. The residue at 850°C was increased by 5.6 wt % when 5 wt % MB was added and 8.1 wt % when 10 wt % MB was added. When LS and MB were added in EP/LS/5MB the decomposition was characterized by the superposition of the effects observed for LS and 5 MB. The beginning of decomposition occurred at temperatures 92°C lower than EP, which is exactly the sum of the LS and MB

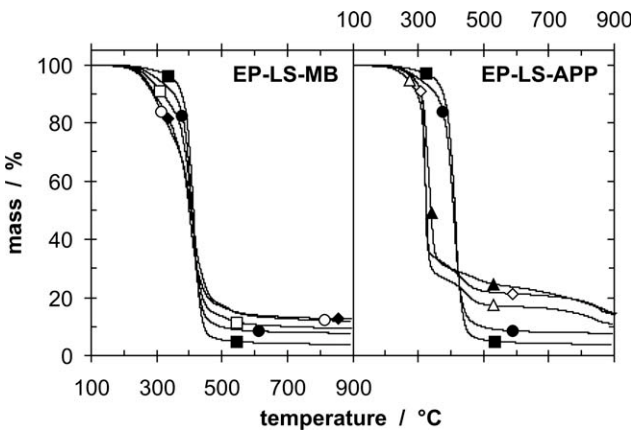

Figure 2 Mass plotted against temperature (heating rate 10°C min^{-1}) under nitrogen of EP (filled squares), EP/LS (filled circles), EP/5MB (squares), EP/LS/5MB (filled rhombi), and EP/10MB (circles) on the left (EP-LS-MB); and EP (filled squares), EP/LS (filled circles), EP/10APP (triangles), EP/LS/10APP (filled triangles), and EP/15APP (rhombi) on the right (EP-LS-APP).

TABLE II
Thermal Decomposition (Thermogravimetry Under Nitrogen; Heating Rate = 10°C min^{-1}); Mass Loss = ML

			ML/%	Residue/%
	$T_{5\%}$/°C	T_{max}/°C	1st + 2nd step	500°C/ 850°C
	± 1°C	± 1°C	± 1%	± 1%/ ± 1%
EP	368	410	89.5	5.4/3.9
EP/LS	346	407	85.3	9.8/7.7
EP/5MB	298	411	87.1	13.5/9.5
EP/LS/5MB	276	402	84.4	16.9/12.7
EP/10MB	278	405	85.3	17.4/12.0
EP/10APP	283	322	84.9	17.6/12.6
EP/LS/10APP	296	326	78.3	25.5/16.7
EP/15APP	303	325	83.3	22.2/16.5

effects. The increase in residue of EP/LS/5MB was roughly what is expected by summing up the impact of LS and MB.

Adding APP clearly changes the decomposition characteristics of the EP (Fig. 2). The main ML step was shifted to temperatures about 88°C lower and the corresponding ML was reduced to around 65–70 wt %. A second subsequent ML step (around 10–15 wt %) occurred up to 500–550°C, and a third high-temperature ML step above 700°C (Fig. 2). The decomposition was changed from one-step decomposition to a multistep one. The FTIR spectrum for the volatiles during the main mass loss clearly showed additional signals, mainly at 3452 cm^{-1}, 1759 cm^{-1}, and 1326 cm^{-1} (amides). No signals of ammonia occurred. The signals of phenolic derivatives increased. The residue at 500°C increased by 12.2 wt % for EP/10APP and 16.8 wt % for EP/15APP; at 850°C it increased by 8.7 wt % and 12.6 wt %, respectively. Combining LS and 10 wt % APP in EP/LS/10APP resulted in a synergism with respect to the residue of 25.5 wt % observed at 500°C. This is higher than what is expected by summing up the impact of LS and APP. The high-temperature residue at 850°C was observed in the form of a superposition.

Based on these results a decomposition model was proposed to describe and summarize the important characteristics of the pyrolysis (Fig. 3). The decomposition of EP (Fig. 3 in the middle) is initiated by the release of butandioic acid and subsequent release of phenolic or carbonylic species. CO_2, CO, or CH_4 are decomposition products of minor decomposition

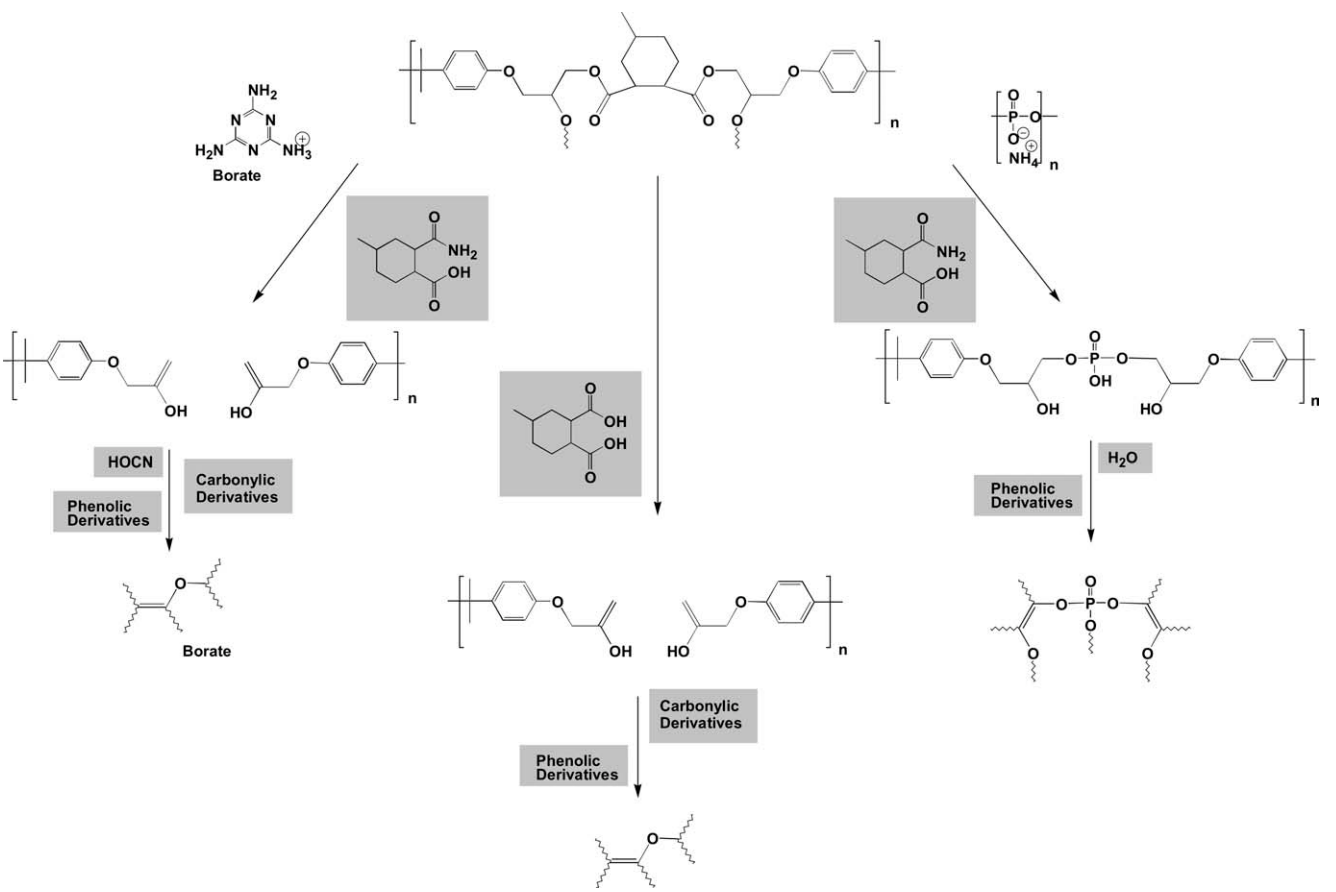

Figure 3 Major decomposition pathway of EP (in the middle), EP/MB (left), and EP/APP (right); observed decomposition products in gray.

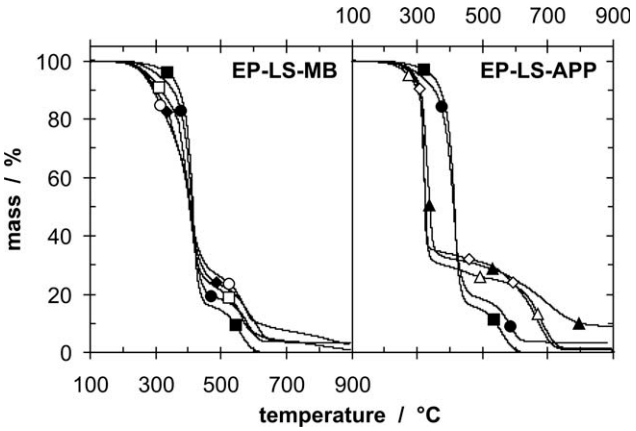

Figure 4 Mass plotted against temperature (heating rate 10°C min^{-1}) under air of EP (filled squares), EP/LS (filled circles), EP/5MB (squares), EP/LS/5MB (filled rhombi), and EP/10MB (circles) on the left (EP-LS-MB); and EP (filled squares), EP/LS (filled circles), EP/10APP (triangles), EP/LS/10APP (filled triangles), and EP/15APP (rhombi) on the right (EP-LS-APP).

pathways, such as the decarboxylation reaction of the dicarbonic acid or fragmentation of CH_4 from bisphenol A species. These reactions were not considered in the model shown in Figure 3. The formation of volatile, saturated decomposition products is accompanied by a small amount of carbonaceous char remaining as residue. LS does not influence the decomposition of EP significantly. In the presence of the nitrogen-containing additives the decomposition of EP is influenced by the decomposition of the additives and the resulting interaction with the EP matrix. Adding melamine borate results in an aminolysis reaction (left pathway in Fig. 3), observed through the release of amide species and isocyanic acid to the gas phase. The residue formation is not effected. Adding APP also resulted in an aminolysis reaction. In contrast to MB, the phosphate of APP is incorporated in the EP network and induces the release of water (right pathway in Fig. 3). Char formation is enhanced. LS in EP/LS/5MB and in EP/LS/10APP does not influence the decomposition significantly.

Thermo-oxidative decomposition

Under air EP decomposes in one major decomposition step and a subsequent smaller one, with a mass loss (ML) of around 80 wt % and around 15 wt % (Fig. 4 and Table III). The T_{max} of the major decomposition step was similar to the thermal decomposition; the subsequent decomposition occurred at T_{max} = 556°C. There was no residue at 850°C. Adding LS to EP has a minor influence on the thermo-oxidative decomposition of the EP. Only the beginning of decomposition was enhanced, shown by the reduction in $T_{5\%}$ of 26°C, whereas T_{max} was not changed. The inorganic part of LS resulted in an increase in residue of around 3.9–3.4 wt %. Apart from the impact on the beginning of decomposition LS behaves like an inert filler in EP. Also, adding MB mainly influences the beginning of the decomposition. $T_{5\%}$ was decreased by 63°C for EP/5MB and 81°C for EP/10MB, respectively, whereas T_{max} was observed around 10°C lower than for EP decomposition. The residue at 500°C was increased by 6.9 wt % when 5 wt % MB was added and 11.5 wt % when 10 wt % MB was added. The residue at 850°C was increased by 1.5 wt % when 5 wt % MB were added and by 3.8 wt % with 10 wt % MB. 3.6 wt %. EP/LS/5MB is characterized by the effects of both LS and MB, but each resulting effect was somewhat less than would be expected for a perfect superposition.

Adding APP clearly changes the thermo-oxidative decomposition of the EP. The main ML step was shifted to temperatures about 94°C lower and the accompanying ML was reduced to around 65–70 wt %. The second subsequent ML step occurred at significantly higher temperatures (Fig. 4), so that around 25 wt % of the char formed in the main decomposition step was stable for more than 200°C. The residue at 500°C was increased by more than 10 wt % for EP/10APP and more than 15 wt % for EP/15APP. Combining LS and 10 wt % APP in EP/LS/10APP results in a thermo-oxidative decomposition very similar to EP/10APP, but with an additional 4 wt % residue at 500°C and an additional

TABLE III
Thermo-Oxidative Decomposition (Thermogravimetry Under Air, Heating Rate = 10°C min^{-1}); Mass Loss = ML

	$T_{5\%}$/°C	T_{max}/°C	ML/%	T_{max2}/°C	ML_2/%	Residue/%
	±1°C	±1°C	±1%	±1°C	±1%	500°C/850°C ±1%/ ±2%
EP	360	416	82.8	556	14.6	14.3/0.0
EP/LS	334	413	83.6	585	14.7	18.2/3.4
EP/5MB	297	407	75.8	565	19.9	21.2/1.5
EP/LS/5MB	286	406	74.2	573	19.1	23.1/3.3
EP/10MB	279	408	70,8	571	23.2	25.8/3.8
EP/10APP	289	322	67.1	685	28.7	25.8/1.3
EP/LS/10APP	307	333	63.1	695	22.1	29.7/9.2
EP/15APP	308	323	62.7	682	33.0	30.8/0.8

TABLE IV
Fire Behaviour (LOI, Ul 94 and Cone Calorimeter). Apart from the Time to Ignition (t_{ig}) the Cone Calorimeter Results Are Averaged Using All of the Measurements at Different Irradiances

				Cone calorimeter		
	LOI/ %	UL 94	t_{ig} (35 kW m^{-2}) / s	THE/ M J m^{-2}	THE/ML/ M J g^{-1} m^{-2}	Residue (%)
Sample	±1		±3	±10	±0.2	±2
EP	20.5	HB	102	140	2.4	5.0
EP/LS	21.2	HB	90	130	2.3	9.2
EP/5MB	23.3	HB	60	142	2.4	9.8
EP/LS/5MB	23.5	HB	60	135	2.4	12.5
EP/10MB	24.1	HB	53	129	2.3	12.0
EP/10APP	23.8	HB	62	105	1.9	15.6
EP/LS/10APP	21.9	HB	63	116	2.2	21.1
EP/15APP	28.9	V0	66	84	2.0	35.3[a]

[a] the results for EP/15APP depend significantly on the irradiance used, so that the average is only a rough estimation for the values between 24.3% and 53.1%.

8 wt % residue at 850°C. This latter value may indicate a synergy.

The impact of LS, MB, and APP on the fire behavior of EP

LS works mainly as an inert filler that yields an inorganic-carbonaceous protection surface layer when burning EP/LS. Adding LS resulted in limited additional residue of around 4 wt % (Table IV), corresponding to the inert silicate added. The residue of EP and EP/LS corresponded well to the residue found for the thermal decomposition. No additional carbonaceous char was obtained. The effective heat of combustion of the volatile decomposition products (THE/ML) did not show a significant change because of the absence of flame inhibition. But EP/LS showed a pronounced barrier effect (Figs. 5 and 6), decreasing the peak heat release rate (PHRR) in the cone calorimeter test in particular. The efficiency of this fire retardancy mechanism differed strongly with respect to fire properties and different fire scenarios. The most impressive reduction occurred for flame spread in high-irradiation scenarios, such as the PHRR in the cone calorimeter (Fig. 6). The other minor effects were hardly relevant (Table IV). The influence of other fire characteristics like flammability (no significant increase in LOI) and THE (decrease around 7%) was hardly significant, and thus insufficient (no vertical classification in UL 94). Only the melt flow and particular the dripping in the UL 94 was inhibited. Burning EP specimen showed melt flow and dripping in vertical UL 94 after a while, most probably when intermediate liquid decomposition products reached a critical amount or concentration. Adding LS to the materials worked as an efficient antidripping agent. The time to ignition (t_{ig}) was even worsened. EP/LS behaves like a typical nanocomposite in which a very large reduction in PHRR and a change in melt viscosity of the pyrolysing material is accompanied by insufficient overall flame retardancy.[10,15] Like other nanocomposite systems, EP/LS must be combined with another flame retardant in order to achieve flame retardant materials.

Quite similar to LS, in the cone calorimeter MB worked mainly as inert filler that forms a protection surface layer when EP/5MB and EP/10MB are burned. Adding MB induced limited additional carbonaceous residue formation of the polymer matrix, of around 2–3 wt % when 5 wt % MB and 10 wt % MB were added (Table IV). The effective heat of combustion of the volatile decomposition products (THE/ML) did not change because of the absence of flame inhibition. Whereas, EP/5MB and EP/10MB showed a pronounced barrier effect (Figs. 5 and 6), decreasing the PHRR in the cone calorimeter test in

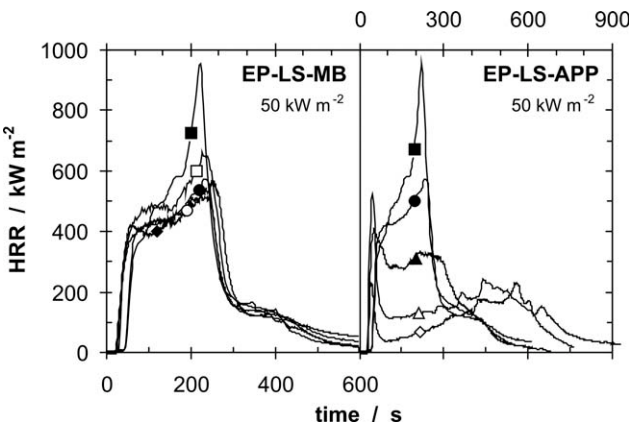

Figure 5 Heat release rate (HRR) plotted against time (irradiance 50 kW m^{-2}) of EP (filled squares), EP/LS (filled circles), EP/5MB (squares), EP/LS/5MB (filled rhombi), and EP/10MB (circles) on the left (EP-LS-MB); and EP (filled squares), EP/LS (filled circles), EP/10APP (triangles), EP/LS/10APP (filled triangles), and EP/15APP (rhombi) on the right (EP-LS-APP).

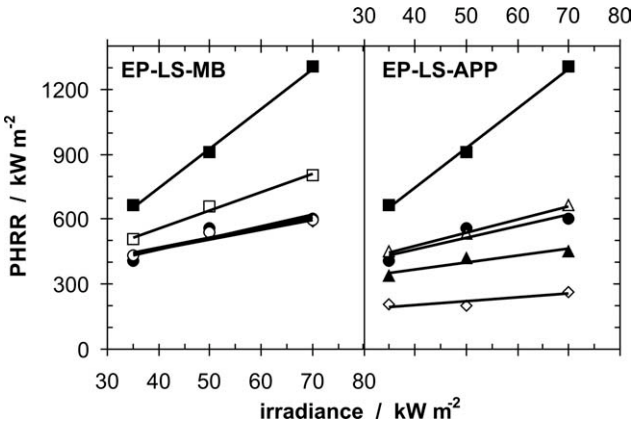

Figure 6 Peak heat release rate (PHRR) plotted against irradiance of EP (filled squares), EP/LS (filled circles), EP/5MB (squares), EP/LS/5MB (filled rhombi), and EP/10MB (circles) on the left (EP-LS-MB); and EP (filled squares), EP/LS (filled circles), EP/10APP (triangles), EP/LS/10APP (filled triangles), and EP/15APP (rhombi) on the right (EP-LS-APP).

particular. The efficiency of this fire retardancy mechanism differed strongly with respect to fire properties and different fire scenarios. The most impressive reduction occurs for flame spread in high-irradiation scenarios, such as the PHRR in the cone calorimeter (Fig. 6). Hereby, adding 10 wt % MB resulted in exactly the same flame retardance effect as 5 wt % LS. 5 wt % MB was not as effective as 5 wt % LS in the cone calorimeter. Also, similarly to LS, the THE was influenced insufficiently and the time to ignition (t_{ig}) was worsened. However, adding 5 and 10 wt % MB improved the LOI by around 2.8 and 3.5%, respectively, significantly more than the corresponding effect observed for LS. Analogous leveling-off of the flame retardancy effect was also observed for the reduction in PHRR. The flame retardancy caused by MB is not linear with MB content, so that it is not promising to use higher amounts of MB to achieve better flame retardance. Further, the improvement observed in flammability is not sufficient to achieve a V-classification in the UL 94. Thus, the combination with another flame retardant is an obvious demand for MB.

When APP was added, the carbonaceous char yield was increased (Table IV). APP induces intumescent behavior in EP/APP and the char built up a voluminous cone structure more than 3 cm high. After ignition a large initial peak in HRR occurred until the insulating intumescent surface layer was built up, followed by a very low HRR (Fig. 5). Hence, the burning time was prolonged extensively. The HRR showed a second maximum when material got too close to the cone heater.[44,46] The THE/ML was decreased (Table IV), probably because of fuel dilution by non-combustible gas and some phosphorus released in the flame, resulting in flame inhibition. Apart from the reduction in PHRR and HRR, the effect of adding 10 wt % APP was not convincing (increase of 3.3% in LOI and no vertical classification in UL 94), whereas 15 wt % APP turned out to be a real flame retardant in EP with respect to the performance demanded for applications. The LOI was increased by 8.3%, the THE was decreased by 40%, and the char yield was 5 to 10 times than that of EP. A V0 classification was achieved in UL 94. Comparing the impact of 10 and 15 wt % APP, it becomes clear that there is no linear relationship between the flame retardancy effect and the APP content. This is quite typical for intumescent systems.[40] Only above a threshold content does the intumescent layer turn from a good heat barrier reducing the HRR into an effective insulation that protects underlying material from reaching the pyrolysis temperature. The sample becomes self-extinguishing before the entire combustible polymer is consumed. This effect was more pronounced for low external heat flux than for high ones, which is shown clearly in the char yield of between 24 and 53 wt % observed in the cone calorimeter. It can not be observed in the reduction in PHRR at the beginning of burning. Flame retardants that become increasingly sufficient with high amounts are obvious candidates for use together with synergists or adjuvants to decrease their threshold value to facilitate commercial use.

The impact of combining LS and MB on the fire behavior of EP

The combination of layered silicate (5 wt %) and MB (5 wt %) in EP/LS/5MB shows antagonism with respect to the HRR, THR and LOI (Figs. 5 and 6, Table IV). Actually there is no significant difference in the HRR observed upon adding EP/LS, EP/LS/5MB and EP/10MB. The residue of EP/LS/5MB is greater than the residue of EP/LS or EP/5MB, respectively, but also slightly less than expected for a real superposition of the effects. The time to ignition seems to be dominated by the addition of MB and thus clearly worsened. With respect to flammability (LOI) EP/5MB, EP/LS/5MB, and EP/10MB show similar results. Further V0 classification in UL 94 was not achieved. There is no linear relationship between the reduction by MB and the amount of MB, but some leveling-off with higher amounts of MB. Thus, comparing EP/LS/5MB with the EP/LS and EP/5MB indicated a larger antagonism than when it is compared with EP/LS and EP/10MB. However, there is no benefit observed for using the combination of LS and MB. The results contrast with the superposition in PHRR reduction reported when 5 wt % layered silicate and zinc borate are used in polyamide 6,[47]

Figure 7 Fire residue of EP+15 wt % APP (on left) and EP+LS+10 wt % APP (on right). Combining APP with LS influences the intumescence and quantity of the char. The illustrated inhibition of intumescence is concluded to cause the antagonism in EP+LS+10 wt % APP. [Color figure can be viewed in the online issue, which is available at www.interscience.wiley.com.]

indicating that the general conclusion depends on the investigated system.

The impact of combining LS and APP on the fire behavior of EP

The combination of layered silicate (5 wt %) and APP (10 wt %) in EP/LS/10APP shows clear antagonism with respect to the HRR, THR and LOI (Figs. 5 and 6, Table IV). The shape of the HRR curve seems to be right in between the behaviors observed for adding LS and APP, respectively, and thus does not show a superposition. The reduction in the PHRR of EP/LS/10APP was clearly less than the simple superposition of the reductions observed when LS and APP were added (Fig. 6). The combination reduced the barrier effect because of APP. The PHRR was observed in the order: EP > EP/10APP = EP/LS > EP/LS/10APP > EP/15APP. The LOI was observed in the order: EP < EP/LS < EP/LS/10APP < EP/10APP < EP/15APP, with only EP/15APP achieving a V0 classification in UL 94. There is no linear relationship between the reduction by APP and the amount of APP. Thus, comparing EP/LS/10APP with the EP/LS and EP/10APP indicated a smaller antagonism than when it is compared with EP/LS and EP/15APP. The same antagonism occurred for THE, which was observed in the order: EP > EP/LS > EP/LS/10 APP = EP/10APP > EP/15APP. The main fire retardancy mechanism of APP, intumescence, was strongly inhibited by adding LS (Fig. 7). It is concluded that the increased melt viscosity of decomposition products reduces the deformation of the residue. The crucial impact of LS on the melt viscosity of the pyrolysing EP was already discussed for the melt flow and dripping behavior of EP and EP/LS in the UL 94 test. Efficient intumescence is observed when the viscosity is small enough for the residue to expand, and large enough to fix the bubbles in a foam-like structure. Thus, an adjustment of viscosity is demanded. Adding LS to polymer/APP systems influences the viscosity in the pyrolysis zone, the residue amount and the mechanical strength of the fire residue. These interactions can be deleterious[48] as in the investigated system, but can also be advantageous.[32] depending on the systems investigated and fire test used. However, in the investigated system the intumescence was clearly inhibited and performance worsened. Also, the flammability showed a clear antagonism for the investigated system (Table IV).

CONCLUSIONS

The fire behavior of EP/LS nanocomposites was investigated when LS was combined with two flame retardants, MB and APP, that also act via a surface protection layer. In particular the question was addressed as to whether the surface effects enhance or compete with each other and thus result in a synergy or antagonism.

The glassy coating because of 10 wt % MB during combustion showed effects similar to 5 wt % nanodispersed LS in the cone calorimeter test and somewhat better flame retardancy in flammability tests, such as LOI and UL 94. The combination of 5 wt % LS and 5 wt % MB shows a clear antagonism. Using EP/LS/5MB is not superior to EP/LS or EP/10MB. The combination of LS and MB in EP/LS/5MB did not result in an optimization of the carbonaceous-inorganic surface layer, such as a more closed surface.

Adding APP in EP/10APP and EP/15APP resulted in intumescent systems. In particular, the fire retardancy was convincing when 15 wt % APP was used with a low external heat flux and thus also in flammability tests like LOI and UL 94. V0 classification was achieved when 15 wt % APP was used in EP/15APP. Combining 5 wt % LS with 10 wt % APP results in strong antagonism in the

investigated fire properties because of inhibiting intumescence, most probably through an increase in melt viscosity of the pyrolysing materials. Intumescent surface protection layers are built only when the viscosity is adjusted correspondingly. In the investigated system, adding LS in EP/LS/10APP most probably resulted in a too high viscosity, killing the intumescence.

The flame retardancy efficiency of the formed protection layers does not increase linearly with higher concentrations of additives. MB indicated some leveling-off with increasing amounts, whereas APP indicated a threshold value for excellent flame retardancy. Comparing EP/LS/5MB with EP/5MB reveals a larger antagonism than with EP/10MB. Comparing EP/LS/10APP with EP/10APP reveals a smaller antagonism than comparing with EP/15APP.

The combination of different halogen-free additives is widely used as a way to achieve a sufficient flame retardance level that cannot be reached by increasing the amount of additives or using the small amounts of flame retardant desired. However, the performance of the investigated combinations of LS with the flame retardants MB and APP was disappointing. The investigated combinations of flame retardants that work through surface protection layers do not yield valuable superposition or synergy, but significant antagonism in the investigated systems. Furthermore, no novel promising approach was indicated towards real halogen-free flame retarded EP.

References

1. Gilman, J. W.; Kashiwagi, T.; Lichtenhan, J. D. SAMPE J 1997, 33, 40.
2. Kojima, Y.; Usuki, A.; Kawasumi, M.; Okada, A.; Fukushima, Y.; Karauchi, T.; Kamigaito, O. J Polym Sci Part A: Polym Chem 1993, 31, 983.
3. LeBaron, P. C.; Wang, Z.; Pinnavaia, T. J Appl Clay Sci 1999, 15, 11.
4. Schartel, B.; Wendorff, J. H. Polym Eng Sci 1999, 39, 128.
5. Morgan, A. B.; Wilkie, C. A., Eds. Flame Retardant Polymer Nanocomposites, Wiley: Hoboken, 2007.
6. Gilman, J. W. In Flame Retardant Polymer Nanocomposites, Morgan, A. B., Wilkie, C. A., Eds.; Wiley: Hoboken, 2007; Chapter 3, 67–87.
7. Kashiwagi, T.; Harris, R. H.; Zhang, X.; Briber, R. M.; Cipriano, B. H.; Raghavan, S. R.; Awad, W. H.; Shields, J. R. Polymer 2004, 45, 881.
8. Gilman, J. W.; Harris, R. H.; Shields, J. R.; Kashiwagi, T.; Morgan, A. B. Polym Adv Technol 2006, 17, 263.
9. Zanetti, M.; Kashiwagi, T.; Falqui, L.; Camino, G. Chem Mater 2002, 14, 881.
10. Bartholmai, M.; Schartel, B. Polym Adv Technol 2004, 15, 355.
11. Schartel, B.; Pötschke, P.; Knoll, U.; Abdel-Goad, M. Eur Polym J 2005, 41, 1061.
12. Kashiwagi, T.; Mu, M.; Winey, K.; Cipriano, B.; Raghavan, S. R.; Pack, S.; Rafailovich, M.; Yang, Y.; Grulke, E.; Shields, J.; Harris, R.; Douglas, J. Polymer 2008, 49, 4358.
13. Schartel, B.; Weiß, A. Fire Mater, in press; DOI: 10.1002/fam.1007.
14. Schartel, B.; Weiß, A.; Sturm, H.; Kleemeier, M.; Hartwig, A.; Vogt, C.; Fischer, R. X. Polym Adv Technol, in press. DOI: 10.1002/pat.1644.
15. Schartel, B.; Bartholmai, M.; Knoll, U. Polym Adv Technol 2006, 17, 772.
16. Gilman, J. W.; Kashiwagi, T. In Polymer-Clay Nanocomposites, Pinnavaia, T. J., Beall, G. W., Eds.; Wiley: Chichester, 2000; Chapter 10, 193–206.
17. Bourbigot, S.; Duquesne, S.; Jama, C. Macromol Symp 2006, 233, 180.
18. Morgan, A. B. Polym Adv Technol 2006, 17, 206.
19. Schartel, B.; Knoll, U.; Hartwig, A.; Pütz, D. Polym Adv Technol 2006, 17, 281.
20. Bödiger, M.; Eckel, T.; Wittmann, D.; Alberts, H. Ger. Pat. DE 19530200A1 (1997).
21. Schall, N.; Engelhardt, T.; Simmler-Hübenthal, H.; Beyer, G. Ger. Pat. DE 19921472A1 (2000).
22. Eckel, T.; Ooms, P.; Wittmann, D.; Buysch, H.-J. Ger. Pat. DE 4231774A1 (1994).
23. Klatt, M.; Grutke, S.; Heitz, T.; Rauschenberger, V.; Plesnivy, T.; Wolf, P.; Jwünsch, J. R.; Fischer, M. Ger. Pat. DE 19705998 A1 (1998).
24. Klatt, M.; Grutke, S.; Heitz, T.; Rauschenberger, V.; Plesnivy, T.; Wolf, P.; Jwünsch, J. R.; Fischer, M. Ger. Pat. DE 19714900 A1 (1998).
25. Eckel, T.; Zobel, M.; Wittmann, D. Ger. Pat. DE 19828536 A 1 (1999).
26. Chigwada, G.; Wilkie, C. A. Polym Degrad Stab 2003, 81, 551.
27. Chigwada, G.; Jash, P.; Jiang, D. D.; Wilkie, C. A. Polym Degrad Stab 2005, 89, 85.
28. Toldy, A.; Toth, N.; Anna, P.; Keglevich, G.; Kiss, K.; Marosi, G. Polym Adv Technol 2006, 17, 778.
29. Hussain, M.; Varley, R. J.; Mathys, Z.; Cheng, Y. B.; Simon, G. P. J Appl Polym Sci 2004, 91, 1233.
30. Le Bras, M.; Bourbigot, S. Fire Mater 1996, 20, 39.
31. Bourbigot, S.; Le Bras, M.; Dabrowski, F.; Gilman, J. W.; Kashiwagi, T. Fire Mater 2000, 24, 201.
32. Bourbigot, S.; Le Bras, M.; S. Duquesne, S.; M. Rochery, M. Macromol Mater Eng 2004, 289, 499.
33. Beyer, G. Fire Mater 2001, 25, 193.
34. Zhang, J.; Wilkie, C. A. Polym Adv Technol 2005, 16, 549.
35. Beyer, G. J Fire Sci 2005, 23, 75.
36. Zanetti, M.; Camino, G.; Canavese, D.; Morgan, A. B.; Lamelas, F. J.; Wilkie, C. A. Chem Mater 2002, 14, 189.
37. Gianelli, W.; Camino, G.; Tabuani, D.; Bortolon, V.; Savadori, T.; Monticelli, O. Fire Mater 2006, 30, 333.
38. Hartwig, A.; Pütz, D.; Schartel, B.; Bartholmai, M.; Wendschuh-Josties, M. Macromol Chem Phys 2003, 204, 2247.
39. Hartwig, A.; Sebald, M.; Kleemeier, M. Polymer 2005, 46, 2029.
40. Eckel, T. In Plastics Flammability Handbook, 3rd ed., Troitzsch, J., Ed.; Hanser: Munich, 2004; Chapter 5.2, pp 158–172.
41. Zhu, J.; Morgan, A. B.; Lamelas, F. J.; Wilkie, C. A. Chem Mater 2001, 13, 3774.
42. Xie, W.; Xie, R. C.; Pan, W. P.; Hunter, D.; Koene, B.; Tan, L. S.; Vaia, R. Chem Mater 2002, 14, 4837.
43. Kunze, R.; Schartel, B.; Bartholmai, M.; Neubert, D.; Schriever, R. J Therm Anal Cal 2002, 70, 897.
44. Schartel, B.; Hull, T. R. Fire Mater 2007, 31, 327.
45. Schartel, B. In Flame Retardant Polymer Nanocomposites, Morgan, A. B., Wilkie, C. A., Eds. Wiley: Hoboken, 2007; Chapter 3, pp 67–87.
46. Schartel, B.; Bartholmai, M.; Knoll, U. Polym Degrad Stab 2005, 88, 540.
47. Shanmuganathan, K.; Deodhar, S.; Dembsey, N.; Fan, Q.; Calvert, P. D.; Warner, S. B.; Patra, P. K. J Appl Polym Sci 2007, 104, 1540.
48. Bertelli, G.; Marchetti, E.; Camino, G.; Costa, L.; Locatelli, R. Angew Makromol Chem 1989, 172, 153.